

# Reduction of the Casimir force from indium tin oxide film by UV treatment

C.-C. Chang,<sup>1</sup> A. A. Banishev,<sup>1</sup> G. L. Klimchitskaya,<sup>2</sup>

V. M. Mostepanenko,<sup>3</sup> and U. Mohideen<sup>1</sup>

<sup>1</sup>*Department of Physics and Astronomy,*

*University of California, Riverside, California 92521, USA*

<sup>2</sup>*North-West Technical University, Millionnaya Street 5, St.Petersburg, 191065, Russia*

<sup>3</sup>*Noncommercial Partnership “Scientific Instruments”,*

*Tverskaya Street 11, Moscow, 103905, Russia*

## Abstract

A significant decrease in the magnitude of the Casimir force (from 21% to 35%) was observed after an indium tin oxide (ITO) sample interacting with an Au sphere was subjected to the UV treatment. Measurements were performed by using an atomic force microscope (AFM) in high vacuum. The experimental results are compared with theory, and a hypothetical explanation for the observed phenomenon is proposed.

PACS numbers: 12.20.Fv, 78.66.-w, 78.20.-e, 12.20.Ds

The Casimir effect [1] is important in various fields from condensed matter physics and nanotechnology to atomic physics and the theory of fundamental interactions [2–8]. Recent experimental progress [9] has allowed alteration of the magnitude of the Casimir force by using test bodies made of materials other than metals. This is of major importance for the problem of stiction [3] in microelectromechanical devices, where it is desirable to make all background forces as small as possible. Thus, it was demonstrated [10, 11] that the Casimir force between an Au sphere and a Si plate is smaller by 25%–40% in comparison with the case of two Au test bodies. For a plate made of ITO interacting with an Au sphere, the gradient of the Casimir force was shown [12] to be roughly 40%–50% smaller than between an Au sphere and an Au plate. For an Au sphere interacting with AgInSbTe plate the gradient of the Casimir force decreases in magnitude by approximately 20% when the crystalline plate is replaced with an amorphous plate [13]. The gradient of the Casimir force between an Au sphere and a semimetallic plate was measured to be about 25%–35% smaller than that for both Au bodies [14]. In addition, the increase in magnitude of the Casimir force between an Au sphere and a Si plate by a few percent was observed when the plate was illuminated with laser pulses [15]. In all these cases measured changes in the force were produced by respective modifications in the optical properties of plates.

In this Letter we report a striking phenomenon of a pronounced decrease in the magnitude of the Casimir force between an Au-coated sphere and ITO film deposited on a quartz substrate after the film undergoes a UV treatment. It is surprising that the observed decrease is not associated with corresponding modification in the optical properties of the film sufficient for changing the Casimir force in accordance with the Lifshitz theory. The hypothetical explanation of this phenomenon, which could find multidisciplinary applications, is provided.

Measurements of the Casimir force were performed using a modified multimode AFM. It was placed in a high vacuum chamber. Only oil free mechanical and turbo pumps were used to obtain the vacuum. The experiments were done at a pressure of  $10^{-6}$  Torr. The AFM was modified to be free of volatile organics. To have a low vibration noise environment, we used an optical table and a sand damper box to prevent coupling of the low frequency noise from the mechanical and turbo pumps. To stabilize the AFM laser used for the detection of cantilever deflection, we employed a liquid nitrogen cooling system, which maintained the temperature of the AFM at 2°C. The cooling system reduced the laser noise and drift. It

also served as an additional cryo pump to obtain the high vacuum.

A polystyrene sphere was glued with silver epoxy ( $20\ \mu\text{m} \times 20\ \mu\text{m}$  spot) to the tip of a triangle silicon nitride cantilever with a nominal spring constant  $\sim 0.01\ \text{N/m}$ . The cantilever-sphere system was then coated with a 10 nm Cr layer, followed by 20 nm Al layer and finally with a  $105 \pm 1\ \text{nm}$  Au layer in an oil free thermal evaporator with a  $10^{-7}$  Torr vacuum. To make sure that the Au surface is smooth, the coatings were done at a very low deposition rate of  $3.75\ \text{\AA}/\text{min}$ . The radius of Au sphere was determined using a SEM to be  $101.23 \pm 0.5\ \mu\text{m}$  after the end of the force measurements.

The ITO films were prepared by RF sputtering (Thinfilms Inc.) on a 1 cm square single crystal quartz plates of 1 mm thickness. A film thickness was measured to be  $74.6 \pm 0.2\ \text{nm}$ . The nominal film resistivity is  $42\ \Omega/\text{sq}$ . The ITO film on the quartz plate was cleaned with the following procedure: First, the plate was immersed in acetone and cleaned in an ultrasonic bath for 15 min. It was then rinsed 3 times in DI water. This ultrasonic cleaning procedure and water rinsing was repeated next with methanol followed by ethanol. After ethanol cleaning the sample was dried in a flow of pure nitrogen gas. Next, electrical contacts to copper wires were made by soldering with indium wire. Then the force measurements described below were performed. Thereafter the same sample was UV treated, and the measurements were repeated.

To prepare the UV-treated sample, the ITO film on a quartz plate was placed in a special air chamber containing a UV lamp. A pen-ray Mercury lamp with a length of 9.0" and outside diameter of 0.375" was used as the UV source. The lamp emits a spectrum with the primary peak at 254 nm ( $5.4\ \text{mW}/\text{cm}^2$  at 1.9 cm distance) and a secondary peak at 365 nm ( $0.2\ \text{mW}/\text{cm}^2$  at 1.9 cm distance). The sample was placed 1 cm from the lamp for 12 hours. The UV-treated sample was cleaned as above. The roughness profiles of the Au coating on the sphere and the ITO film were measured with an AFM (the variances are 3.17 and 2.28 nm, respectively).

The measurement procedure is as follows. The samples were inserted on top of the AFM piezo and placed in the high vacuum chamber. The ITO film was connected to voltage supply (33120A, Agilent Inc.) operating with  $1\ \mu\text{V}$  resolution. A  $1\ \text{k}\Omega$  resistor was connected in the series with the voltage supply to prevent surge currents and protect the sample surface during sphere-plate contact. The cantilever-sphere system was mounted on the AFM head which was connected to the ground. To reduce the electrical noise, care was taken to make

Ohmic contacts and eliminate all Schottky barriers, to the ITO plate and Au sphere. To minimize electrical ground loops all the electrical ground connections were unified to the AFM ground. Ten different voltages  $V_i$  ( $i = 1, 2, \dots, 10$ ) in the range from  $-260$  to  $-100$  mV (from  $-25$  to  $150$  mV for the UV-treated sample) were applied to the plate, while the sphere remained grounded.

The total force  $F_{\text{tot}}$  (electrostatic plus Casimir) between the Au sphere and the ITO plate was measured as a function of sphere-plate separation. A  $0.05$  Hz continuous triangular voltage was applied to the AFM piezo to change the separations between the sphere and the plate by  $2 \mu\text{m}$ . The interferometric calibration of the piezo was done as discussed previously [16, 17]. Starting at the maximum separation, the plate was moved towards the sphere and the corresponding cantilever deflection was recorded every  $0.2$  nm till the plate contacted the sphere. The sphere-plate separation  $a$  is given by:

$$a = z_{\text{piezo}} + S_{\text{def}}m + z_0, \quad (1)$$

where  $z_{\text{piezo}}$  is the movement of the plate due to the piezo, the product of deflection signal  $S_{\text{def}}$  and deflection coefficient  $m$  is the change in separation distance due to cantilever deflection, and  $z_0$  is the average separation on contact due to surface roughness.

After the contact of the sphere and the plate, the cantilever-sphere system vibrates with a large amplitude. To allow time for this vibration to damp out, a  $5$  s delay was introduced after every cycle of data acquisition. The total force measurement was repeated 10 times for every applied voltage.

The electrostatic calibration was performed as follows. The total force is given by  $F_{\text{tot}} = kmS_{\text{def}}$ , where  $k$  is cantilever spring constant. Any linear deflection with sphere-plate separation due to mechanical drift of the photodetector was first subtracted. For separations larger than  $1.7 \mu\text{m}$ , the total force between the sphere and the plate is below the instrumental sensitivity. The small observed deflection from the region  $1.7$ – $2 \mu\text{m}$  was fitted to a straight line and the coefficients were used to subtract this drift from the whole force curve for all separations. The sphere-plate contact was corrected for mechanical drift and the cantilever deflection coefficient  $m = 104.4 \pm 0.5$  nm per unit deflection signal and  $m = 103.5 \pm 0.6$  nm per unit deflection signal was determined as discussed in Ref. [18] for the untreated and UV-treated samples, respectively. These values of  $m$  were used to determine the sphere-plate separation  $a$  in Eq. (1) up to the value of  $z_0$  (which is a constant for the

complete set of measurements).

The residual potential difference  $V_0$  between the Au sphere and ITO plate, the spring constant  $k$  and the average separation on contact  $z_0$  were determined from the parabolic dependence of the total force on the applied voltage. The cantilever deflection at every applied voltage was determined at intervals of 1 nm sphere-plate separations using linear interpolation. For each separation the  $S_{\text{def}}$  was plotted as a function of the applied voltage. From the parabolas generated, the residual potential  $V_0$ , which corresponds to the value of the voltage for zero electrostatic force at the vertex of the parabola, was determined by a least  $\chi^2$  fitting procedure. The values  $V_0 = -196.8 \pm 1.5$  mV for untreated and  $V_0 = 65 \pm 2$  mV for UV-treated sample were found to be independent of separation. The curvature of the parabola was also determined at every separation  $a$ . This curvature as a function of the sphere-plate separation was fitted to the spatial-dependent part of the electrostatic force to obtain the average separation on contact and the spring constant. As a result,  $z_0 = 29.5 \pm 0.4$  nm,  $k = 0.0139 \pm 0.0001$  N/m for the untreated sample, and  $z_0 = 29 \pm 0.6$  nm,  $k = 0.0138 \pm 0.0001$  N/m for the UV-treated sample. These values of  $z_0$  were used to determine absolute separations from Eq. (1). The values of  $k$  and  $m$  were used to convert the measured  $S_{\text{def}}$  to values of force.

Using the above procedure, we have measured the total force at each of the applied voltages  $V_i$  over the separation region from 60 to 300 nm with a step of 1 nm. This measurement was repeated ten times resulting in one hundred values of the total force  $F_{ik}^{\text{tot}}(a)$  ( $k = 1, 2, \dots, 10$ ) at each separation.

The systematic error in the values of total force measured,  $\Delta_s F_{ik}^{\text{tot}}(a)$ , is added from the separation-dependent calibration error and the instrumental noise including background noise level which does not depend on separation. The resulting  $\Delta_s F_{ik}^{\text{tot}}(a)$  is equal to 2.1, 1.5, and 1.1 pN at  $a = 60, 100$  and  $\geq 200$  nm, respectively (all errors here and below are determined at a 95% confidence level).

The values of the Casimir force at each separation were obtained by the subtraction of the electric force in the sphere-plate geometry [2]

$$F_{ik}(a) = F_{ik}^{\text{tot}}(a) - 2\pi\epsilon_0(V - V_0)^2 \sum_{n=1}^{\infty} \frac{\coth \alpha - n \coth n\alpha}{\sinh n\alpha}, \quad (2)$$

where  $\cosh \alpha = 1 + a/R$ , and  $\epsilon_0$  is the permittivity of vacuum. The systematic errors in the electric force are determined by the errors in  $V_0$ ,  $R$  and, primarily, in  $a$ . The resulting

systematic error of the Casimir force, was found from the combination of errors in the total and electric forces. The variance of the mean Casimir force from 100 repetitions does not depend on  $a$  and is equal to 0.55 pN. Then from the Student distribution the random error was obtained, which was combined with the systematic error to find the total experimental error,  $\Delta^{\text{tot}}F(a)$ , in the measured Casimir force.

In Fig. 1, the mean Casimir force measured as a function of separation is shown as crosses for an untreated and UV-treated ITO films (lower and upper sets of crosses, respectively). The arms of the crosses indicate the total experimental errors in the measurement of separations and forces. To illustrate, in the inset to Fig. 2 we plot  $\Delta^{\text{tot}}F(a)$  for the UV-treated sample as a function of separation. The lower set of crosses in Fig. 1 indicates a 40%–50% decrease in the force magnitude as compared to the case of two Au bodies (e.g., at  $a = 80$  nm the measured force is  $-144$  pN in comparison with  $-269$  pN), in agreement with Ref. [12].

From Fig. 1 it can be seen that the magnitude of the Casimir force from the UV-treated film is markedly less than from the untreated one. The relative decrease in the force magnitude is equal to 21% at  $a = 60$  nm, increases to approximately 35% at  $a = 130$  nm, and preserves this value at larger separations. Measurements were repeated several times with different samples, untreated and UV-treated, leading to similar results.

The measurement results were compared with computations using the Lifshitz theory at the experimental temperature  $2^\circ\text{C}$  for an ITO film on a quartz substrate interacting with an Au sphere, and the proximity force approximation (PFA). The error in using the PFA for real materials with given experimental parameters does not exceed 0.3% [19–21]. The roughness of both ITO and Au surfaces was taken into account by means of geometrical averaging [2, 9]. The resulting correction to the force is equal to 2.2% at  $a = 80$  nm, and becomes less than 1% and 0.5% at  $a \geq 90$  nm and  $a \geq 116$  nm, respectively. The dielectric properties of ITO films were investigated using the untreated and UV-treated samples prepared in the same way and under the same conditions as those used in measurements of the Casimir force. The imaginary part of  $\varepsilon_{\text{ITO}}(\omega)$  was determined [22] in the frequency region from 0.04 eV to 8.27 eV with IR-VASE and VUV-VASE ellipsometers at low and high frequencies, respectively. The results for  $\text{Im}\varepsilon$  are shown in the insets to Fig. 3(a,b) by the solid lines for untreated and UV-treated samples, respectively. They were extrapolated to lower frequencies by the Drude model with the plasma frequency  $\omega_p = 1.5$  eV and relaxation parameters  $\gamma = 0.128$  eV and  $\gamma = 0.132$  eV. The dashed lines in the insets show the limits of a possible smooth

extrapolation of the measured optical data to higher frequencies obtained from the oscillator model. As can be seen in the insets,  $\text{Im } \varepsilon_{\text{ITO}}$  is only slightly affected by the UV treatment. The respective dielectric permittivities along the imaginary frequency axis,  $\varepsilon_{\text{ITO}}(i\xi)$ , are shown in main part of Fig. 3(a,b) by solid and dashed lines. Here, the dashed [in Fig. 3(a)] and solid [in Fig. 3(b)] lines indicate  $\varepsilon_{\text{ITO}}(i\xi)$  with the role of charge carriers neglected. For quartz, the  $\varepsilon(i\xi)$  of Ref. [23] was used. The optical properties of Au were taken from Ref. [24] and extrapolated to lower frequencies by means of the Drude model with  $\omega_p = 9.0$  eV and  $\gamma = 0.035$  eV (this extrapolation nicely fits [25] the measured data [24]).

The theoretical results are shown by the lower and upper bands between the pairs of solid lines in the inset to Fig. 1 for the untreated and UV-treated samples, respectively. In computations, we have used the pairs of solid lines in both Figs. 3(a) and (b), i.e., neglected the contribution of charge carriers in the UV-treated film. In the main field of Fig. 2, we repeat the experimental data for the UV-treated sample, but show the theoretical results computed using the dashed lines in Fig. 3(b), i.e., with account of charge carriers. As can be seen in Figs. 1 and 2, the data are in excellent agreement with theory with charge carriers of the UV-treated sample neglected, but at a 95% confidence level exclude the theory taking these charge carriers into account. Note that the same results are obtained when Au is described by the generalized plasma-like model [2, 9]. One can hypothesize that the UV-treatment resulted in the transition of an ITO film to a dielectric state without noticeable change of its optical properties at room temperature (according to Ref. [26], the UV-treatment of ITO leads to lower mobility of charge carriers). This hypothesis could be verified in future by the investigation of electrical properties at very low temperature. Then, the neglect of charge carriers for a UV-treated sample fits commonly accepted practice in the application of the Lifshitz theory to dielectric bodies [2, 9].

In the foregoing, we have experimentally demonstrated that the UV-treatment of an ITO sample interacting with an Au sphere leads to an overall decrease of the Casimir force up to 65% in comparison to Au-Au test bodies. This result is of much practical importance for addressing problems of lubrication and stiction in microelectromechanical systems. The hypothetical explanation of the observed phenomenon provided invites further investigation of the physical properties of complicated chemical compounds including their interaction with zero-point and thermal fluctuations of the electromagnetic field.

This work was supported by the DARPA Grant under Contract No. S-000354 (equipment,

A.B., U.M.), NSF Grant No. PHY0970161 (C.-C.C, G.L.K., V.M.M., U.M.) and DOE Grant No. DEF010204ER46131 (G.L.K., V.M.M., U.M.).

---

- [1] H. B. G. Casimir, Proc. K. Ned. Akad. Wet. B **51**, 793 (1948).
- [2] M. Bordag, G. L. Klimchitskaya, U. Mohideen, and V. M. Mostepanenko, *Advances in the Casimir Effect* (Oxford University Press, Oxford, 2009).
- [3] E. Buks and M. L. Roukes, Phys. Rev. B **63**, 033402 (2001).
- [4] A. W. Rodriguez, F. Capasso, and S. G. Johnson, Nature Photon. **5**, 211 (2011).
- [5] A. Ashourvan, M. Miri, and R. Golestanian, Phys. Rev. Lett. **98**, 140801 (2007).
- [6] H. B. Chan et al., Phys. Rev. Lett. **101**, 030401 (2008).
- [7] J. F. Babb, Adv. At. Mol. Opt. Phys. **59**, 1 (2010).
- [8] E. G. Adelberger, B. R. Heckel, and A. E. Nelson, Ann. Rev. Nucl. Part. Sci. **53**, 77 (2003).
- [9] G. L. Klimchitskaya, U. Mohideen, and V. M. Mostepanenko, Rev. Mod. Phys. **81**, 1827 (2009); Int. J. Mod. Phys. B **25**, 171 (2011).
- [10] F. Chen et al., Phys. Rev. A **72**, 020101(R) (2005); **74**, 022103 (2006).
- [11] F. Chen et al., Phys. Rev. Lett. **97**, 170402 (2006).
- [12] S. de Man et al., Phys. Rev. Lett. **103**, 040402 (2009); S. de Man, K. Heeck and D. Iannuzzi, Phys. Rev. A **82**, 062512 (2010).
- [13] G. Torricelli et al., Phys. Rev. A **82**, 010101(R) (2010).
- [14] G. Torricelli et al., Europhys. Lett. **93**, 51001 (2011).
- [15] F. Chen et al., Optics Express **15**, 4823 (2007); Phys. Rev. B **76**, 035338 (2007).
- [16] F. Chen and U. Mohideen, Rev. Sci. Instrum. **72**, 3100 (2001).
- [17] H. E. Grecco and O. E. Martinez, Appl. Opt. **41**, 6646 (2002).
- [18] H.-C. Chiu et al., J. Phys. A **41**, 164022 (2008).
- [19] A. Canaguier-Durand et al., Phys. Rev. Lett. **104**, 040403 (2010).
- [20] R. Zandi, T. Emig, and U. Mohideen, Phys. Rev. B **81**, 195423 (2010).
- [21] B. Geyer, G. L. Klimchitskaya, and V. M. Mostepanenko, Phys. Rev. A **82**, 032513 (2010).
- [22] <http://www.jawoollam.com>
- [23] L. Bergström, Adv. Coll. Interface Sci. **70**, 125 (1997).
- [24] *Handbook of Optical Constants of Solids*, ed. E. D. Palik (Academic, New York, 1985).

[25] G. Bimonte, Phys. Rev. A **83**, 042109 (2011).

[26] C. N. Li et al., Appl. Phys. A **80**, 301 (2005).

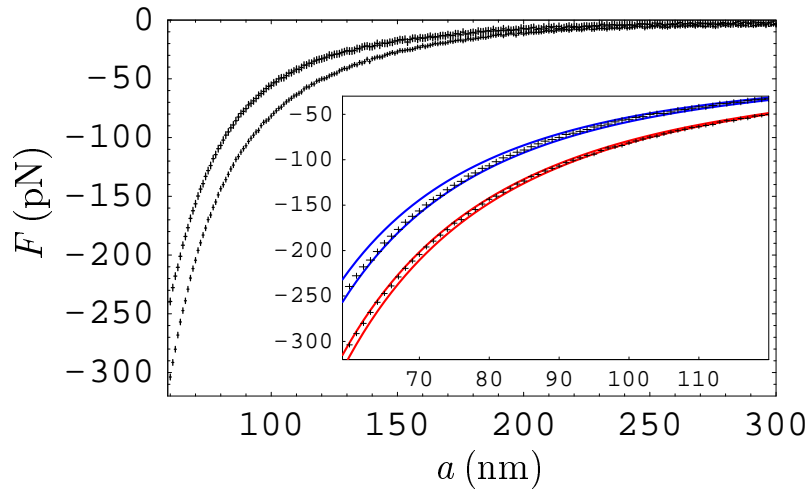


FIG. 1: The mean measured Casimir forces between an Au sphere and untreated and UV-treated ITO samples as functions of separation are shown by the lower and upper sets of crosses, respectively. In the inset the same data are compared with theory (see text for further discussion).

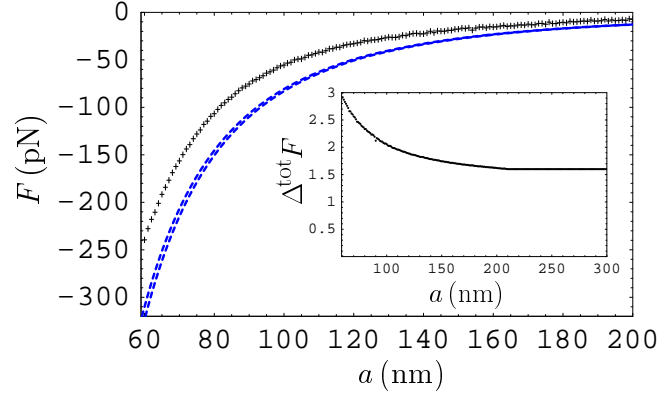


FIG. 2: The measured Casimir force between an Au sphere and an UV-treated ITO sample as functions of separation is shown as crosses. The band between the dashed lines indicates the theoretical prediction where the ITO charge carriers are described by the Drude model. In the inset, the dependence of the total experimental error on separation is plotted.

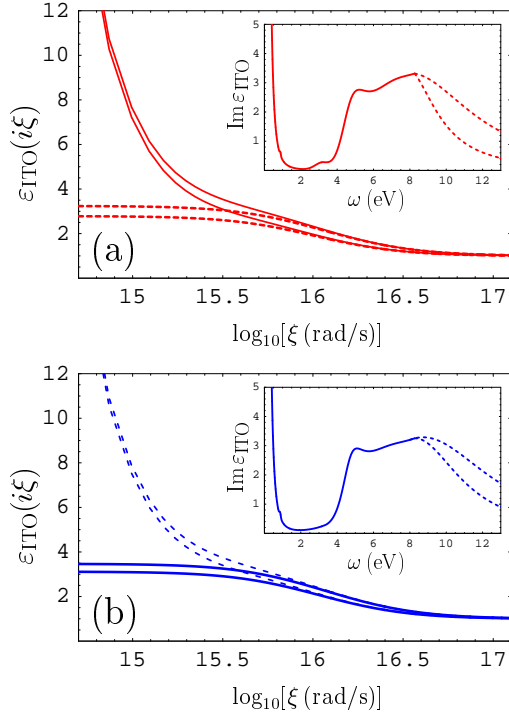


FIG. 3: The dielectric permittivities as a function of imaginary frequency are shown (a) for a untreated ITO sample with charge carriers included (solid lines) and neglected (dashed lines) and (b) for a UV-treated sample with charge carriers included (dashed lines) and neglected (solid lines). In the insets the imaginary parts of corresponding dielectric permittivities obtained from ellipsometry are presented.